Rev. Roum. Sci. Techn.– Électrotechn. et Énerg.
Vol. **62**, *1*, pp. 3–7, Bucarest, 2017

NEW SOLUTION OF LINEAR DC ACTUATOR WITH ADDITIONAL PERMANENT MAGNETS: WORKING PRINCIPLE, DESIGN AND TESTING

ALEXANDRU RĂDULIAN[1], MIHAI MARICARU[2], IOSIF VASILE NEMOIANU[2], RADU CREȚU[3]

Key words: Linear dc actuator, Ne-Fe-B permanent magnets, Vacuum circuit breakers (VCB), High actuating force, High holding force, Efficiency, Compactness, Reliability, Cost efficiency.

The paper presents the principle of a dc high-force compact actuator for operating vacuum circuit breakers. By using properly placed Ne-Fe-B permanent magnets, the actuator we propose has the following advantages: it is able to perform a large number of mechanical operation cycles (at least one million) with high frequency rate and high holding force in closed position. Through reducing air gaps and leakage fluxes and the introduction of permanent magnets in the magnetic circuit, the proposed technical solution ensures low power consumption, compactness, reliability and reduced manufacturing cost. Such a linear actuator proves to be versatile finding application in operating valves remotely, robotic systems, packaging machines, electric switchgears, medical equipment, production machinery *etc*. Least but not last, it may find application in transportation industry ranging from rail to aircraft equipment. The working principle of the actuator is presented, followed by preliminary calculations and finite element simulations (static and dynamic) in FEMM package, incorporating specially designed LUA scripts. Finally, measurements performed on an actuator prototype are presented and discussed.

1. **INTRODUCTION**

Vacuum circuit breakers (VCBs) are today's preferred technical solution to the obsolete sulphur hexafluoride (SF_6) gas technology in medium voltage range. The main reason is the feature of vacuum to be an electric arc extinguishing medium. When VCB contacts open, an electric arc appears as a result of ionization of metal vapors belonging to contacts, in the context of the extreme temperatures occurring at that stage. Rapid condensing of these ionized particles back to the contacts' surface ensures an efficient regain of the dielectric strength specific to an arc quenching medium. Apart from this important physical characteristic of VCBs, it is worth to mention that SF_6 gas circuit breakers present a significantly larger greenhouse effect than CO_2 itself, and therefore its use is increasingly limited in recent years. Moreover, an arc extinguished in SF_6 gas will produce toxic fumes which may cause health issues to the operation and maintenance personnel. Therefore, abandoning the SF_6 circuit breakers in medium voltage grids operation has become a visible trend in recent years, followed by a logical expected increase in VCBs use.

The force necessary to separate the VCB contacts is provided either by stored mechanical energy (*e. g.* preloaded springs) or by an electromagnetic linear actuated device. A linear actuator has the advantage of being more robust and thus more reliable compared to the mechanically stored energy devices, allowing a significantly larger number of operations and also a reduced packaging. Consequently, it requires less maintenance having a reduced number of moving parts and thus ensures less expensive operation costs. Normally, a linear actuator would not require any maintenance at all during its entire lifespan [1].

Electromagnetic parameters of such a device are more controllable than those of a mechanically stored device. On that basis, during the last decade, linear actuators have become increasingly used in circuit breaking technical applications [2].

The present study focuses on a particular design of a such linear actuator, which will provide better operation parameters, such as holding force, response time *etc*. The main idea is to introduce strong Ne-Fe-B permanent magnets into the classical design with the purpose of improving the mechanical parameters of the actuator, in order to better respond to the operation parameters required by the VCB as an electric arc quenching device.

Section 2 presents the main proposed design improvements along with the preliminary calculation of the actuator's components and parameters: geometry, rated coil voltage and current, number of coil turns *etc*.

Section 3 is dedicated to the finite element method (FEM) model of the device and its simulation carried out in FEMM software package [3].

The performed simulations not only allow a more accurate and refined computation than the estimate results mentioned in Section 2, but also a calculation of the force acting on the mobile armature of the device, as performed in Section 4.

A prototype of the actuator is presented in Section 5, along with experimental setup and determinations of its operating performances.

In Section 6, final conclusions are drawn and discussed.

2. **PROPOSED LINEAR ACTUATOR DESIGN**

Our linear actuator design is intended for the use in a three-phase VCB rated for a voltage of 126 kV, a rated current of 2 500 A and a rated breaking current for short-circuit of 40 kA. Additionally, the following design imposed characteristics are considered:

- minimum force at maximum air gap: 3,000 N;
- maximum force at minimum air gap: 6,000 N;
- stroke length: 80 ± 2 mm;

[1] ICPE, Spl. Unirii 313, 030138 Bucharest, Romania
[2] "Politehnica" University of Bucharest, Faculty of Electrical Engineering, Department of Electrical Engineering, 313 Splaiul Independenței, 060042 Bucharest, Romania, E-mail: mihai.maricaru@upb.ro, iosif.nemoianu@upb.ro
[3] "Politehnica" University of Bucharest, Faculty of Electrical Engineering, BSc graduate

- minimum air gap: 0.1 mm;
- rated coil voltage: 200 – 400 Vcc;
- ambient temperature: 40° C;
- coil over temperature (with respect to ambient temperature): 40° C.

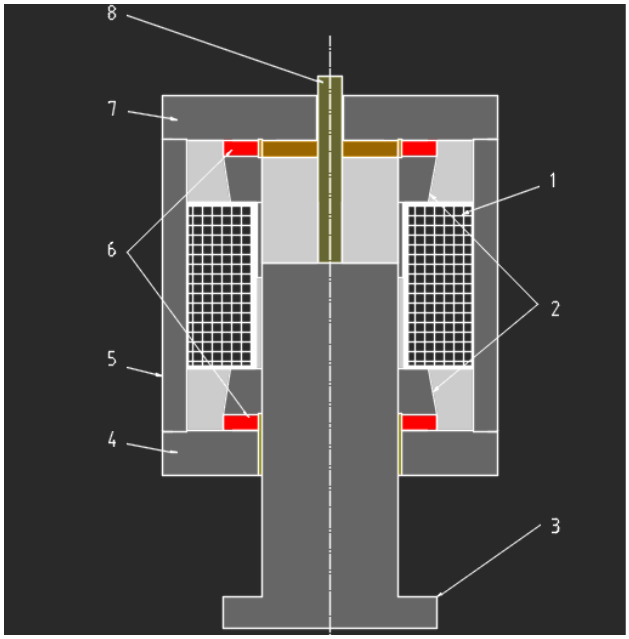

Fig. 1 – Linear actuator cross sectional geometry.

Preliminary calculations provide an estimated number of 3,000 turns, 15 A rated current intensity, 125 mm height and 40 mm width for the coil parameters. The obtained coil wire diameter is 1.291 mm with a resistivity of $2.19 \cdot 10^{-8}$ Ωm. The air gap flux density becomes in open position (for stroke length) 0.495 T.

The actuator's cross sectional geometry is shown in Fig. 1, corresponding to a cylindrical symmetry structure. The numbered parts depicted in Fig. 1 are as follows:

1 – electromagnet coil;
2 – intermediate pole pieces;
3 – mobile armature;
4 – lower pole piece;
5 – middle pole piece;
6 – Ne-Fe-B permanent magnets;
7 – upper pole piece;
8 – guide shaft.

The actuator's electromagnet is made up by a central cylindrical polar piece 5, which houses the coil 1, composed of two windings (not shown distinctively in Fig. 1): a closing one (of inductance L_i) and an opening one (of inductance L_d) – see Fig. 2. Inside 1, guided by the lower and upper lids (polar pieces 4 and 5, respectively), ensuring concentricity through the guide shaft 8, travels the mobile armature 3. To be noted the introduction of the upper and lower Ne-Fe-B permanent magnets 6 (pairing the lower and upper lids 4 and 7), whose role is to provide the actuator's holding force in open and closed positions, without being assisted by supplementary dc fed coils. That technical solution saves the energy that otherwise would have been spent by the supplementary coils, improving thus the overall efficiency of the device. Later, it will be tested the possible omission of one of the two magnets, in order to reduce the overall manufacturing cost. The intermediate polar pieces 2 mechanically hold together the lower and upper lids (4 and 7) and their pairing permanent magnets 6. Polar pieces 2 have the additional role to better channel the magnetic flux lines toward the air gap in order to ensure greater magnitudes of the generated dynamic forces necessary to operate the VCB, according with its mechanical specifications [4].

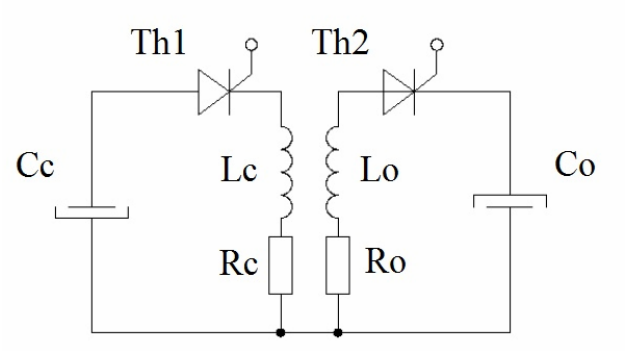

Fig. 2 – Schematic diagram of the electronic driver.

The electronic equivalent circuit driving the actuator is shown in Fig. 2, comprising the following circuit elements:

- C_c – closing capacitor [μF];
- C_o – opening capacitor [μF];
- L_c – closing coil inductance [mH];
- L_o – opening coil impedance [mH];
- R_c – closing coil ohmic resistance [Ω];
- R_o – opening coil ohmic resistance [Ω];
- Th_1 – closing position command thiristor;
- Th_2 – opening position command thiristor.

For energizing the closing coil, the circuit is powered in order to charging capacitor C_c. Then, the closing command opens the thiristor's (Th1) gate allowing the rapid discharge of C_c under the form of a current impulse of several A in intensity, which will flow through the electromagnet's closing coil winding 1 [3].

The magnetic field produced by the rapid discharge current surge through the coil generates an important force acting upon the mobile armature 3, which will travel to the upper pole piece 7. Even after the current impulse vanishes, the mobile armature 3 remains locked onto the upper pole piece 7 as a result of the magnetic field produced by the upper permanent magnets 6, even if there is a resistant force pulling it back (provided by mechanical means, *e.g.* by a spring).

For the opening stage, capacitor C_o is charged with opposite polarity. Similarly, the thiristor's gate opening command produces the rapid discharge of C_o resulting in an important transient current flowing through the opening winding of electromagnet coil 2 [11].

The magnetic field produced by this current is oppositely directed to those of the permanent magnets, so that the resultant field within the air gap separating the mobile armature 3 and the upper lid 7 is extremely weak. Consequently, the developed force within the air gap by the resulting magnetic field will be smaller than the resistant force, and the moving armature 3 travels back to the maximum air gap resting position.

3. FINITE ELEMENT MODEL OF THE ACTUATOR IN FEMM

Several different approaches are possible for solving a nonlinear magnetic problem [5, 6]. Nonetheless, a relatively simple but effective solution may be obtained using the FEMM package. The axisymmetric geometry structure of the actuator allows a significant reduction (by half) of the problem's domain, leading also to roughly half of the mesh points that would correspond to the complete structure, as shown in Fig. 3.

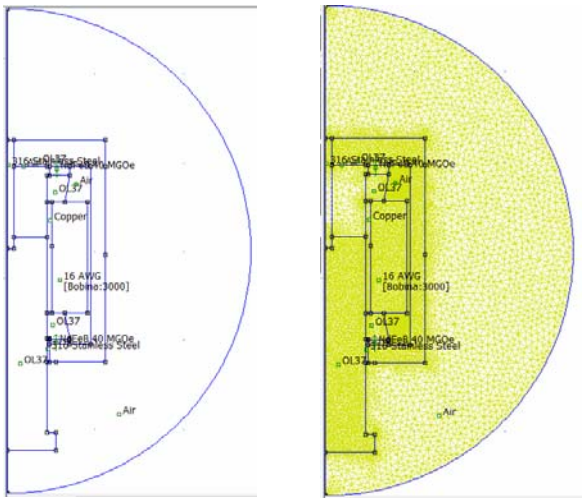

Fig. 3 – FEMM model of the linear actuator (open position – maximum air gap): left – without mesh, right – including generated mesh.

Although the interest area of our study is focused at the interior of the actuator, where in the air gap zone the magnetic force is generated, for a better accuracy of the results we adopted an "open boundary" simulation, corresponding to "impedance" (Robin) boundary conditions.

In order to generate a strong magnetic force over a confined space, we adopted Nd-Fe-B 40 MGOe rare earth strong permanent magnets. According with the preliminary calculus mentioned in Section 2, the closest standardized copper wire is 16 AWG, chosen from the FEMM component library, in which flows a 15 A current [5].

The magnetic circuit considered material is S235JR, whose *B–H* characteristic is shown in Fig. 4. A special attention must be payed to the magnetic characteristic of the core material and to the specific associated losses [7–9].

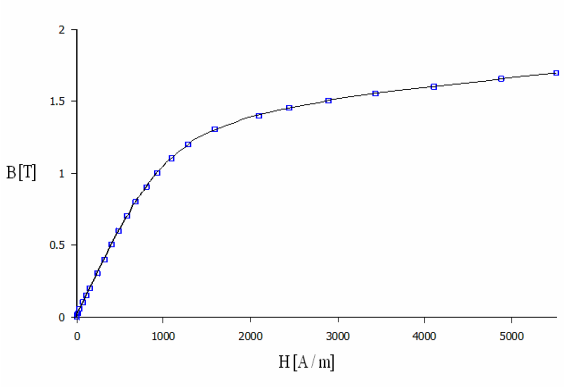

Fig. 4 – *B–H* characteristic of the magnetic circuit material S235JR.

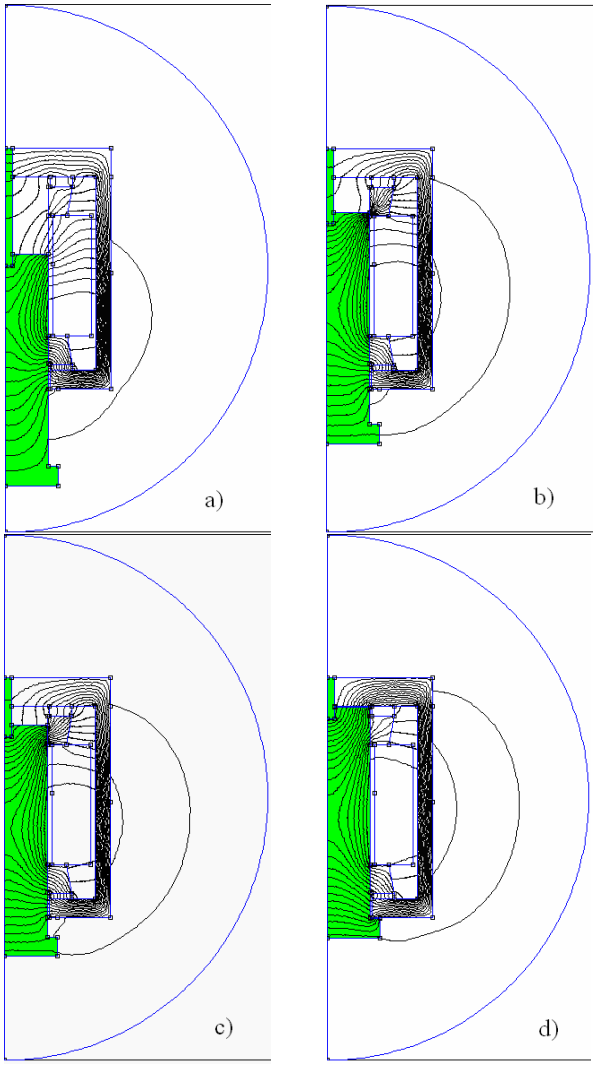

Fig. 5 – Flux density lines for various air gap lengths: a) 80 mm (open position); b) 40 mm; c) 20 mm; d) 0.1 mm (closed position).

A LUA script was generated to solve the field problem obtained by gradually shifting the moving armature *3* with 0.5 mm steps along the upward vertical direction up to the minimum air gap position. At each step the actuating force is computed using Maxwell's stress tensor along the closed contour of the moving armature surface. Additionally, a screen capture of the resulted magnetic field spectrum is exported in BMP format at each step, allowing very useful qualitative interpretations as the moving armature shifts its position.

4. NUMERICAL SIMULATIONS AND RESULTS

The magnetic field lines spectrum is shown in Fig. 5, for several air gap lengths: 80 mm (open position), 40 mm, 20 mm and 0.1 mm (closed position), respectively. It becomes now obvious that the use of Ne-Fe-B permanent magnets is therefore validated because in the open and closed positions, at these ends, there is an intense magnetic field capable of maintaining the armature in the respective position even without being assisted by additional mechanical components.

The choice for the material S235JR is also validated, since one can notice in Fig. 5, the flux leakage is weak outside the actuator's housing.

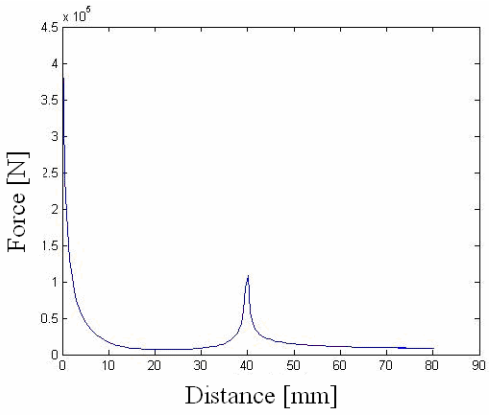

Fig. 6 – Computed force acting on the mobile armature, for an excitation coil of 3 000 turns.

A specially designed LUA script has allowed us to obtain the force acting on the mobile armature at each intermediate step of 0.5 mm, ranging from the open position up to the closed position. The results of the simulations are shown in Fig. 6.

A sudden increase in the force magnitude is to be noticed at half of the actuator's stroke.

5. EXPERIMENTAL RESULTS

To validate the results obtained from the computerized simulation we performed test over a prototype actuator capable of fulfilling the conditions presented in Section 2. Figure 7 shows the prototype of linear dc actuator made of solid steel S235JR coated with a thin layer of zinc. It can be observed that the flanges are combined with the round pipe through four M8 screws. At the end on the left side of the actuator it is mounted a nonmagnetic stroke limiter.

Fig. 7 – The prototype of the proposed linear dc actuator.

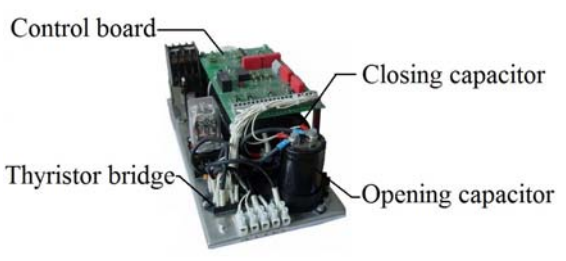

Fig. 8 – The prototype of electronic driver.

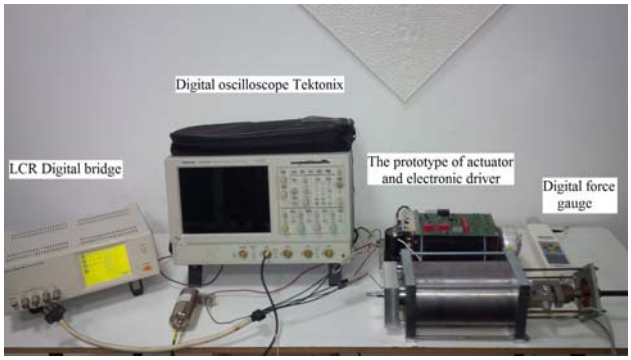

Fig. 9 – Experimental setup of linear dc actuator.

Figure 8 shows the prototype of electronic driver. Constructively, the electronic driver is based on the principle diagram shown in Fig. 2. It is composed of closing capacitor, opening capacitor, thyristor bridge, control and protection devices and a control board. The whole assembly has a compact volume.

Figure 9 shows the experimental setup for measuring the electrical and mechanics parameters of the actuator. The mechanical parameters were measured using a digital force gauge SAUTER FH 10K and velocity and stroke were measured using a Penny & Giles SLS095 linear displacement sensor. The electrical parameters were measured using a digital a LRC digital bridge HIOKI 3532-50 and a digital oscilloscope Tektronix TDS 5104 with ac/dc current probe [10].

The experimental result of the static force in closed position is 5,400 N the result of the simulations is 5,600 N. The results obtained from experimentation and simulation are almost similar with some differences caused by assembly and measurement tolerances [11, 12]. Figure 10 shows the variation of the coil current and the voltage capacitor due to closing operation. The measured value of the current was 15.5 A (Table 1).

Table 1

Results obtained from measurements

Static force in the closed position	5,400 N	
Closing coil inductance	Without magnetic yoke	185.41 mH
	With magnetic yoke	567.07mH
Opening coil inductance	Without magnetic yoke	40.151 mH
	With magnetic yoke	149.3 mH
Closing coil ohmic resistance	9.26 Ω	
Opening coil ohmic resistance	3.94 Ω	
Number of turns	Closing coil	1,069
	Opening coil	3,100
Current	15.5 A	

6. CONCLUSIONS

An improved type of linear actuator for large developed forces is theoretically described and tested. The main idea, which makes the object of a registered patent [4], resides in the presence of two strong Ne-Fe-B ring magnets at the upper and lower positions of the mobile armature. That avoids the intervention of dc coils for producing the magnetic force

necessary to retain the mobile armature in closed and open positions. This solution not only saves power, but also is more robust, proving thus more reliable as a VCB actuating device. FEMM simulation and actual prototype measurement are in good agreement, validating thus both the technical solution and performed calculations.

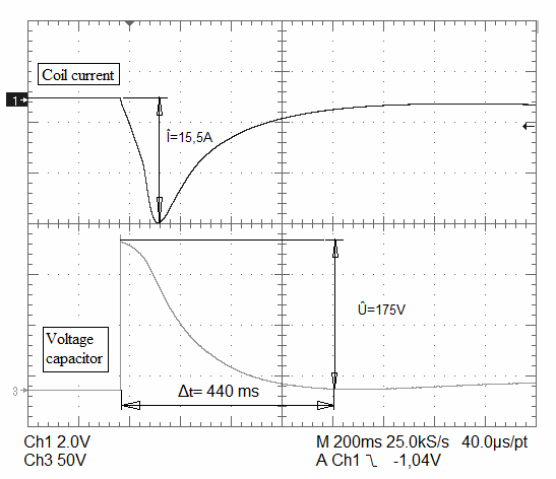

Fig. 10 – Waveforms of the dc current (upper trace) and applied voltage (lower trace).

Further improvements of the design are possible in order to increase the actuating force.

ACKNOWLEDGMENTS

This work was financially supported by the Executive Agency for Higher Education, Research, Development and Innovation Funding through the Financial Agreement PCCA no. 34/2012.

Received on November 24, 2016

REFERENCES

1. A. Radulian, N. Mocioi, I. Deaconu, *Intreruptorul cu comutatie in vid de 145 kV destinat centralelor electrice de 110 kV – solutie ecologica si moderna pentru Romania*, Forumul Regional al Energiei pentru Europa Centrală şi de Est – FOREN 2016, Costinesti, June 12–16, 2016.
2. P. Slade, *The Vacuum Interrupter – Theory, Design and Aplicattion*, CRC Press, NewYork, 2001, pp. 423–430.
3. A. Radulian, *Modelarea unui dispozitiv electromagnetic cu magneţi permanenţi folosind metoda elementului finit*, Revista Electrotehnică, Electronică, Automatică (EEA), **60**, *1*, 2012.
4. A. Radulian, *Electromagnet in hybrid construction with excitation coil and permanent magne*t, Patent No. A 2013 00177.
5. I.R. Ciric, F.I. Hănţilă, M. Maricaru, G.-M. Vasilescu, *A novel approach to the analysis of nonlinear magnetic fields produced by coils with imposed voltages*, Rev. Roum. Sci. Techn. – Électrotechn. et Énerg., **61**, *3*, pp. 213–216, 2016.
6. P. Minciunescu, S. Marinescu, F.I. Hănţilă, O. Drosu, *FEM-BEM technique for solving the magnetic field in electric machines*, Rev. Roum. Sci. Techn. – Électrotechn. et Énerg., **56**, *2*, pp. 189–198, 2011.
7. L. Dumitru, Veronica Păltânea, G. Păltânea, H. Gavrilă, *Magneto-crystalline anisotropy in thin grain oriented silicon iron alloy cut through different technologies*, Rev. Roum. Sci. Techn. – Électrotechn. et Énerg., **61**, *3*, pp. 221–226, 2016.
8. G. Păltânea, Veronica Păltânea, H. Gavrilă, A. Nicolaide, B. Dumitrescu, *Comparison between magnetic industrial frequency properties of non-oriented fesi alloys, cut by mechanical and water jet technologies*, Rev. Roum. Sci. Techn.– Électrotechn. et Énerg., **61**, *2*, pp. 26–31, 2016.
9. V. Manescu (Paltanea), G. Paltanea, H. Gavrila, *Hysteresis model and statistical interpretation of energy losses in non-oriented steels*, Physica B-Condensed Matter, **486**, pp. 12–16, 2016.
10. A. Radulian, N. Mocioi, *Numerical Modelling of an Electromagnetic Actuator for Vacuum Contactors*, International Conference and Exposition on Electrical and Power Engineering – EPE 2014, Iasi, October 2014.
11. N.M. Modreanu, M.I. Andrei, *Numeric Modelling of a Two-Channel Limited Angle Torque Motor*, Revista Electrotehnică, Electronică, Automatică (EEA), **62**, *1*, 2014.
12. D. Pavelescu, E. Ghetea, *Dispozitiv ultrarapid cu repulsie electrodinamica*, Revista Electrotehnică, Electronică, Automatică (EEA), **8**, 1976.